International Journal of Informatics, Information System and Computer Engineering

Image Denoising Method Based on 3D Block Matching with Harmonic Filtering in Transform Domain

Mizanur Rashid, Abdullah Ibne Sayed**, Md Masud Rana***

* School of Electronics and Information Engineering,
Nanjing University of Information Science and Technology, Nanjing, China
** Huazhong University of Science and Technology, Wuhan, China
*Corresponding Email: mizanurrashid218@gmail.com

ABSTRACTS

Today, I will explain an image denoising method based on 3D block matching with harmonic filtering in the transform domain. This topic is important because digital images are susceptible to noise during acquisition, storage, and transmission. Image denoising is crucial in pre-processing and is a key research area in digital image processing and computer vision. Traditional denoising techniques face limitations such as high computational complexity, so combining multiple methods is more effective. The integration of wave-domain harmonic filtering and 3D block matching (BM3D) introduces a new and efficient denoising algorithm. The Euclidean distance approach is used to group similar 2D image blocks into a 3D array. The inverse transformation reconstructs the image, followed by wavelet decomposition to filter high-frequency noise. To prevent edge blurring, the Laplacian-Gaussian algorithm is applied to refine the diffusion model. Finally, wavelet reconstruction is performed to approximate the original image. Experimental results demonstrate that this approach improves information protection and processing speed, making it highly effective in practice.

ARTICLE INFO

Article History:
Received 20 Feb 2025
Revised 01 Mar 2025
Accepted 19 Mar 2025
Available online 15 Apr 2025
Publication date 01 Jun 2026

Keywords:
Image denoising,
Diffusion model,
BM3D,
Laplacian-Gaussian algorithm

DOI: https://doi.org/10.34010/injiiscom.v7i1.15615
p-ISSN 2810-0670 e-ISSN 2775-5584

1. INTRODUCTION

As a common information carrier, digital images are widely used in many social fields such as cultural media, modern industry, military, medicine, agriculture and so on. However, digital images are susceptible to noise in the process of acquisition, storage and transmission. Therefore, image denoising has become an important method in the image pre-processing stage, and is also a recent research hotspot in the field of digital image processing and computer vision (Li & Zhao, 2013).

Various researchers proposed a number of approach to deal with this issue before, here I go through some of the approaches starting with (Buades et al., 2005), he propose the idea of a non-local mean filter using Gaussian white noise in 2005, which is a denoising method to estimate the true image by weighted averaging of similar blocks between neighbourhoods. Later in (Dabov et al., 2007) combined the principles and advantages of NLM algorithm, wavelet transform and Wiener filtering, and proposed a three-dimensional block matching image denoising algorithm (BM3D), At present, which is one of the most obvious algorithms, The high-frequency components obtained from the decomposing of the noise image in proposed by the authors are denoised by using the BM3D algorithm, and finally the wavelet reconstruction is performed, which greatly reduces the computational complexity.

Prior to that in 2006, Hinton published a paper in Science, which showed the team's research on deep learning (Hinton & Salakhutdinov, 2006), and then deep learning began to develop rapidly. In fact, deep learning was first tried in the field of image processing. A neural network model containing a convolutional layer, Convolutional Neural Network (CNN), was proposed by (LeCun, 1989) but this model did not greatly promote this field in image recognition when it was first born. Until 2012, Professor Hinton introduced the weight decay algorithm to optimize this algorithm. During the training process of the neural network, the weight range was better controlled to avoid over-fitting problems in the network. Deepen the network depth of the convolutional neural network (Krizhevsky et al., 2012), so, the convolutional neural network can be better applied to the field of image recognition. In 2015, Zhou et al. introduced a wave-domain harmonic de-noising model for the edge information processing has given very good results (Xian-Xhun et al., 2015). The algorithms proposed by the above scholars all improve to some extent in the peak signal-to-noise ratio test, but they lack a balance in the running speed. Hence, a new method based on block matching collaborative filtering was proposed to estimate the noisy image processing, you can get the basic image estimates (Hwang & Haddad, 1995). Since the noise and the edge details of the image are mainly concentrated in the high frequency part of the image, the high frequency part of the pre-estimation image can be extracted by the wavelet decomposition, the edge blurring is caused by the transformation of the wave field, and the post-reconstruction distortion of the image occurs, Laplacian algorithm (Elmoataz et al., 2012) is used to construct a new operator to bring into the diffusion model for image filtering, and then the final approximation of the image is obtained by wavelet reconstruction.

DOI: https://doi.org/10.34010/injiiscom.v7i1.15615
p-ISSN 2810-0670 e-ISSN 2775-5584

2. IMAGE DENOISING BY MIXING 3D BLOCK MATCHING WITH HARMONIC FILTERING

2.1. BM3D algorithm

This is an ideal denoising approach, that brings together the wavelet transform and local methods. Classed up into two: the initial denoising and final denoising (Elad et al., 2023; Fan et al., 2019). The initial de-noising uses orthogonally transformed windows of different sizes, and the hard threshold of the spectrum in these transforms means that in the approximate class Adaptive decline, and model order depends on the data. The most efficient adaptive sequence estimation is Discrete Cosine Transform (DCT) (Foi et al., 2007). The local estimate becomes nonlocal, when the Euclidean distance is used as a metric to find similar blocks of a reference block. The similar two-dimensional image blocks are combined into a three-dimensional array matrix for joint filtering, then the three-dimensional array is inverse transformed and weighted averagely to eliminate overlapping parts of the image blocks to obtain the pre-estimation of the noisy image (Elmoataz et al., 2012). The final denoising step is to denoise twice based on the initial denoising. Image blocks are grouped again according to the similarities using the weight parameters provided by the initial denoising (Cornelis et al., 2014). The overlapping parts of the image blocks after inverse transformation of the weighted average three-dimensional array get the final estimate of the image (Toprak & Güler, 2006). However, we can see that the denoising methods based on the three-dimensional block matching are based on the image block analysis, lack of grasp of the overall image information.

2.2. Initial estimations

We suppose that the noisy image model is as following according to the theoretical analysis (1):

$$I_{0(x,y)} = I_{(x,y)} + n_{(x,y)}(x, y \grave{o} R) \tag{1}$$

Among them, I_0 denotes a noisy image, I for the original image, n mean 0,Variance is σ^2 Gaussian noise. Assume R is a bounded open subset in the real plane, defined as the domain of the image, is a bounded open subset in the real plane;(x, y) Represents the two-dimensional spatial coordinates of the image field. Definition $x, y \in R$, the reference image block is B_{x_R,y_R}, $B_{x,y}$ For positioning in noisy images $I_{0(x,y)}$, A matching block in the Euclidean distance is used to search for an image similarity block of another region similar to the central pixel region of the current reference block using the Euclidean distance metric as shown in formula (2)

$$d\left(B_{x_R,y_R}, B_{x,y}\right) = N_1^{-2} \left\| \gamma(\Gamma_{2D}\left(B_{x_R,y_R}\right) - \gamma(\Gamma_{2D}\left(B_{x,y}\right)) \right\|_2^2 \tag{2}$$

Assume, B_{x_R,y_R}, $B_{x,y}$ are the size $N_1 \times N_1$ Ima ge blocks, Γ_{2D} Denotes the two-dimension al linear transformation by discrete cosin e (DCT), γ is a threshold operator, and ge nerally defined in (3)

$$\gamma\left(\lambda, \lambda_{thr}\right) = \begin{cases} \lambda & |\lambda| > \lambda_{thr} \\ 0 & |\lambda| \le \lambda_{thr} \end{cases} \tag{3}$$

Define the maximum distance between image blocks to search for similar blocks τ_{match} ,The result of block matching by (4) is:

DOI: https://doi.org/10.34010/injiiscom.v7i1.15615
p-ISSN 2810-0670 e-ISSN 2775-5584

$$S_{x_R,y_R} = \left\{ x,y \in R \middle| d(B_{x_R,y_R}, B_{x,y}) < \tau_{match} \right\} \quad (4)$$

Will be assembled S_{x_R,y_R} Similar blocks in the merged stack as $N_1 \times N_1 \times S_{x_R,y_R}$ The three-dimensional array is normalized by three-dimensional linear transformation of the array, followed by three-dimensional inverse transform to get the initial approximation of the matching block:

$$\hat{I}_{S_{x_R,y_R}} = \Gamma_{3D}^{-1}(\gamma(\Gamma_{3D}(I_{0S_{x_R,y_R}}))) \quad (5)$$

The result of the treatment in equation (5) $\hat{I}_{S_{x_R,y_R}}$ stacked composition $\hat{I}_{x,y}^{x_R,y_R}$ .Where subscripts indicate the position of the estimated block and superscripts indicate the similar block position of the block. Weighted average the pixels of all the image blocks to avoid the overlap of the estimated values (6), so as to obtain the initial approximation of the original image:

$$\hat{I}_{basic} = \frac{\sum_{x,y \in R} \sum_{xm,ym \in S_{x_R,y_R}} \omega_{x_R,y_R} \hat{I}_{xm,ym}^{x_R,y_R}}{\sum_{x,y \in R} \sum_{xm,ym \in S_{x_R,y_R}} \omega_{x_R,y_R} \psi_{xm,ym}} \quad (6)$$

In the formula, $\hat{I}_{basic}$ after processing based on the image, $\psi_{xm,ym}$ Represented as located in (xm, ym) at the block of the characteristic function. ω_{x_R,y_R} Represents the weight assigned to the group estimate, defined as (7), N_{x_R,y_R} for the three-dimensional array of formula (4) to normalize and linear transform the number of non-zero coefficients.

$$\omega_{x_R,y_R} = \begin{cases} \sigma^{-2} N_{x_R,y_R}^{-1} & N_{x_R,y_R} \geq 1 \\ 1 & N_{x_R,y_R} < 1 \end{cases} \quad (7)$$

2.3. Final estimates

The edge and noise features of the image and the edge are mainly concentrated in the high-frequency part of the image. The Mallat algorithm (Mallat, 1989) is used to decompose the result of to extract the high-frequency part of the pre-estimated image (horizontal direction h, vertical Direction v, diagonal direction d), and its diffusion filter processing. Due to Perona-Malik's diffusion function (Perona & Malik, 1990) has edge sharpening capability, it has the function of backward diffusion at the same time of forward diffusion and de-noising as diffusion model. Proposed specific model is as follows:

$$\begin{cases} \frac{\partial I}{\partial t} = div\{c\left[W \times \left(\left|\nabla \hat{I}_{basic}\right|\right)\right] \nabla \hat{I}_{basic}\} \\ \hat{I}_{final}(x,y,0) = \hat{I}_{basic} \end{cases} \quad (8)$$

In the formula, $\hat{I}_{basic}$ is a preliminary estimated image of BM3D, W represents the wavelet transform decomposition of image, and the decreasing function related to gradient information $c[g]$ is used to control the diffusion degree at different positions, which is consistent with the definition of PM model, namely:

$$c(x) = \exp(-\left(\frac{x}{k}\right)^2), \quad (9)$$

Where k is the threshold coefficient. When the wave field is transformed, the edge will be blurred and the edge corners will be easily smoothed, resulting in the distortion of the reconstructed image. The new filter operator can be constructed by using Laplace Gauss's stress distribution balance and gradient operator, its expression is as follows:

DOI: https://doi.org/10.34010/injiiscom.v7i1.15615
p-ISSN 2810-0670 e-ISSN 2775-5584

$$\nabla \hat{I}_{basic} + \nabla^2 \hat{I}_{basic} = \sqrt{I_x^2 + I_y^2} + \frac{\partial^2 I}{\partial x^2} + \frac{\partial^2 I}{\partial y^2} \quad (9)$$

Ta In order to enhance the edge of the image, control the proliferation speed, among them G_σ as Gaussian kernel function.ke (9) into (8) and create a new diffusion model, namely:

$$\begin{cases} \frac{\partial I}{\partial t} = c\left(\left|G_\sigma * \nabla \hat{I}_{basic}\right|\right) div\{c\left[W \times \left(\left|\nabla \hat{I}_{basic} + \nabla^2 \hat{I}_{basic}\right|\right)\right] \nabla \hat{I}_{basic}\} \\ \hat{I}_{final}(x, y, 0) = \hat{I}_{basic} \end{cases} \quad (10)$$

In the formula, $\mathrm{c}(\mathrm{g}) = \mathrm{c}\left(\left|G_\sigma * \nabla \hat{I}_{basic}\right|\right)$.

$$G_\sigma = \frac{1}{\sqrt{2\pi\sigma}} e^{-\frac{\left(x^2+y^2\right)}{4\sigma}} \quad (11)$$

For the model (10) (11) (12), we can simplify the realization of the algorithm by numerical discrete form, and define the grid coordinates as $Net = (il, jl, \Delta t)$,Where l is the grid length, Δt For the time step. Therefore:

$$\begin{cases} I_{i,j}^n = I \cdot Net \\ a_{i,j}^n = \mathrm{c}\left(\left|G_\sigma * \nabla \hat{I}_{basic}\right|\right) \cdot Net \\ b_{i,j}^n = c\left[W \times \left(\left|\nabla \hat{I}_{basic} + \nabla^4 \hat{I}_{basic}\right|\right)\right] \cdot Net \end{cases}$$

definition $I_{basic}^{\sim} = \left[W \times \left(\left|\nabla \hat{I}_{basic} + \nabla^2 \hat{I}_{basic}\right|\right)\right]$,therefore,

$$\begin{aligned} & div\left[c\left(I_{basic}^{\sim}\right) \nabla \hat{I}_{basic}\right] \\ & = \frac{\partial}{\partial x}\left[c\left(I_{basic}^{\sim}\right) \frac{\partial I}{\partial x}\right] + \frac{\partial}{\partial y}\left[c\left(I_{basic}^{\sim}\right) \frac{\partial I}{\partial y}\right] \\ & = \frac{\partial}{\partial x}\left(c\left(I_{basic}^{\sim}\right)\right) \frac{\partial I}{\partial x} + c\left(I_{basic}^{\sim}\right) \frac{\partial^2 I}{\partial x^2} + \frac{\partial}{\partial y}\left(c\left(I_{basic}^{\sim}\right)\right) \frac{\partial I}{\partial y} + c\left(I_{basic}^{\sim}\right) \frac{\partial^2 I}{\partial y^2} \end{aligned} \quad (12)$$

$\frac{\partial I}{\partial x}$ The discrete form is： $\frac{I_{i+1,j} - I_{i-1,j}}{2l}$, $\frac{\partial^2 I}{\partial x^2}$ discrete form is： $\frac{I_{i+1,j} - 2I_{i,j} + I_{i-1,j}}{l^2}$,therefore $\frac{\partial}{\partial x}\left[c\left(I_{basic}^{\sim}\right) \frac{\partial I}{\partial x}\right]$ The discrete expression is:

$$\frac{1}{2l^2}\left[\left(b_{i-1,j}^n + b_{i,j}^n\right) I_{i-1,j}^{n+1} - \left(2b_{i,j}^n + b_{i-1,j}^n + b_{i+1,j}^n\right) I_{i+1,j}^{n+1} + \left(b_{i,j}^n + b_{i+1,j}^n\right) I_{i+1,j}^{n+1}\right] \quad (13)$$

The same can be obtained $\frac{\partial}{\partial y}\left[c\left(I_{basic}^{\sim}\right) \frac{\partial I}{\partial y}\right]$ The discrete expression is：

$$\frac{1}{2l^2}\left[\left(b_{i,j-1}^n + b_{i,j}^n\right) I_{i,j-1}^{n+1} - \left(2b_{i,j}^n + b_{i,j-1}^n + b_{i,j+1}^n\right) I_{i,j+1}^{n+1} + \left(b_{i,j}^n + b_{i,j+1}^n\right) I_{i,j+1}^{n+1}\right] \quad (14)$$

DOI: https://doi.org/10.34010/injiiscom.v7i1.15615
p-ISSN 2810-0670 e-ISSN 2775-5584

The discrete expressions (13), (14) into equation (10) diffusion equation can be obtained implicit difference scheme:

$$\frac{I_{i,j}^{n+1}-I_{i,j}^{n}}{\Delta t}=\frac{1}{2l^2}a_{i,j}^{n}\left[\begin{array}{l}\left(b_{i-1,j}^{n}+b_{i,j}^{n}\right)I_{i-1,j}^{n+1}+\left(b_{i,j-1}^{n}+b_{i,j}^{n}\right)I_{i,j-1}^{n+1}+\left(b_{i,j}^{n}+b_{i+1,j}^{n}\right)I_{i+1,j}^{n+1}\\+\left(b_{i,j}^{n}+b_{i,j+1}^{n}\right)I_{i,j+1}^{n+1}+\left(4b_{i,j}^{n}+b_{i-1,j}^{n}+b_{i,j-1}^{n}+b_{i+1,j}^{n}+b_{i,j+1}^{n}\right)I_{i,j}^{n+1}\end{array}\right] \quad (15)$$

definition $\mathbf{M}_l(I^n)=[a_{ij}(I^n)]$, Write equation (2.15), (2.16), (2.17) into a matrix form and further simplify:

$$\frac{I^{n+1}-I^{n}}{\Delta t}=M_l(I^n)I^{n+1} \quad (16)$$

Which is: $I^{n+1}=\left(1-\Delta t M_l(I^n)\right)^{-1}I^n$ (17)

2.4. Performance analysis

The feasibility of this algorithm is verified by MATLAB simulation software. The PSNR and SSIM are used to compare and evaluate the effectiveness of the proposed algorithm.

$$PSNR=10lg\left(\frac{255^2}{\frac{1}{W\times H}\sum_{x=1}^{W}\sum_{y=1}^{H}[I(x,y)-\hat{I}(x,y)]^2}\right)$$
(18)

$$SSIM=\left[l\left(I,\hat{I}\right)^{\alpha}\cdot c\left(I,\hat{I}\right)^{\beta}\cdot s\left(I,\hat{I}\right)^{\gamma}\right] \quad (19)$$

In formula (18), (19), $W\times H$ Indicates the image size, I, $\hat{I}$ respectively denote the original image and the denoised image, $l(x), c(x), s(x)$ respectively, brightness, contrast, structure comparison function. PSNR the bigger the better, $SSIM\in(0,1)$, the closer this value is to 1, the better the filtering effect.

(a)Nicki (b) Nxb

Fig. 1. The original pictures

Figure 1 shows a natural image Nicki, Nxb. The original experimental chart, pixel size is 512*512.First of all Nicki Images are used separately BLS-GSM、F-NLM、BM3D and this algorithm for smoothing noise. The filtering algorithm in this paper sets the time step $\Delta t=0.2$,The number of iterations $n=7$.Wavelet threshold denoising used sym4 break down. The smoothing result is shown in Figure 2. The upper left corner of the figure is a partial enlarged view. The evaluation indicators are shown in Table 1. Different noise levels can reflect the suppression effect of each model on noise and the retention of edge structure information. The details of the Nicki's eyes and feathers shown in Fig 2, which indicates that the BM3D algorithm has a good visual effect on image detail protection and denoising performance. However, it can be clearly found by comparing the details of the Nxb denoising image in Fig 3. The BM3D algorithm lacks the analysis of the overall information, which leads to the blurring caused by over-processing of partial regions.

DOI: https://doi.org/10.34010/injiiscom.v7i1.15615
p-ISSN 2810-0670 e-ISSN 2775-5584

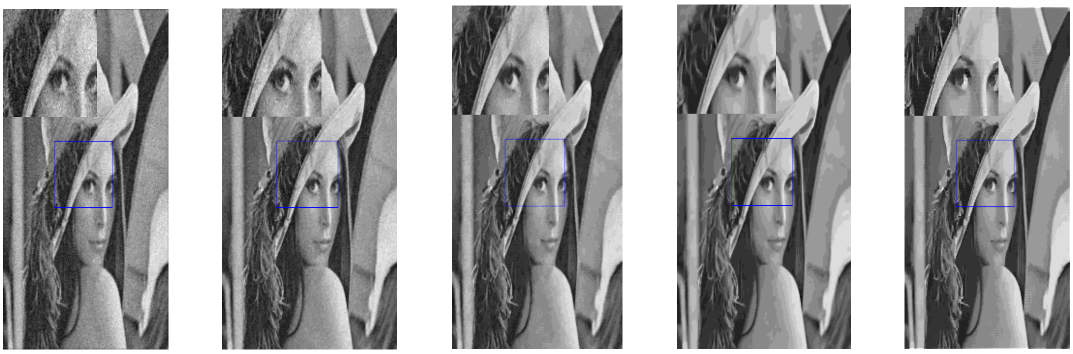

(a)Noisy image (b) BLS-GSM Model (c) F-NLM Model (d)BM3D Model (e) New Model

Fig. 2 The smoothing results of noisy image through different de-noising models (Nicki)

(a)Noisy image (b) BLS-GSM Model (c) F-NLM Model (d)BM3D Model (e) New Model

Fig. 3. The smoothing results of noisy image through different de-noising models (Nxb)

In order to better display the edge information before and after filtering, we use Canny operator (Yuan & Xu, 2015) to detect the edge of the de-noised renderings of each algorithm respectively. The result is shown in Fig 4. Observing the information of the Nicki's brim and feather, the vehicle structure of the lower left corner of the Nxb and the character. The new model proposed in this paper has excellent performance on protecting the detail information structure (Xie et., 2012). By carefully comparing the edges detected from different algorithms, it is evident that the proposed model achieves a better balance between noise suppression and edge preservation. The subtle transitions in the edge regions, such as the feather's fine patterns and the vehicle's contour, are more faithfully retained with this model. The Canny operator highlights how the proposed method minimizes edge degradation that is often seen in traditional denoising techniques. This advantage is particularly significant in areas with complex textures, where maintaining edge continuity is crucial. Overall, the visual analysis confirms the superior capability of the proposed model in handling high-frequency components and preserving structural details.

DOI: https://doi.org/10.34010/injiiscom.v7i1.15615
p-ISSN 2810-0670 e-ISSN 2775-5584

(a)Noisy image (b) BLS-GSM Model (c) F-NLM Model (d)BM3D Model (e) New Model

Fig. 4 Edge extraction noisy images after de-noising in different models

Table 1. PSNR, SSIM and run time of noisy images in different de-noising models

Images	**σ/ PSNR**		**BLS-GSM**	**Fast-NLM**	**BM3D**	**New Model**
Nicki	10/ 28.16	PSNR(dB)	35.22	34.75	35.84	36.11
		SSIM	0.9957	0.9963	0.9981	0.9987
		Time(s)	5.50	4.11	4.12	3.85
	20/ 22.13	PSNR(dB)	30.93	28.14	33.03	33.88
		SSIM	0.93	0.9471	0.9887	0.9981
		Time(s)	5.49	4.58	4.51	3.98
	30/ 18.64	PSNR(dB)	27.84	25.35	31.28	32.09
		SSIM	0.8773	0.8502	0.9765	0.9974
		Time(s)	5.27	4.21	4.71	3.88
	40/ 16.35	PSNR(dB)	25.01	22.85	29.85	29.86
		SSIM	0.7625	0.6455	0.9235	0.9968
		Time(s)	5.25	2.11	3.65	2.84

DOI: https://doi.org/10.34010/injiiscom.v7i1.15615
p-ISSN 2810-0670 e-ISSN 2775-5584

Table 1 (continue). PSNR, SSIM and run time of noisy images in different de-noising models

Images	σ/ PSNR		BLS-GSM	Fast-NLM	BM3D	New Model
Nxb	10/ 28.14	PSNR(dB)	33.13	33.87	34.67	34.88
		SSIM	0.9211	0.8972	0.9667	0.9991
		Time(s)	5.52	4.22	4.04	3.82
	20/ 22.11	PSNR(dB)	29.09	28.22	30.43	32.21
		SSIM	0.8473	0.7835	0.9558	0.9981
		Time(s)	5.39	4.12	4.00	3.87
	30/ 18.59	PSNR(dB)	26.82	22.24	29.21	30.08
		SSIM	0.7773	0.7875	0.9425	0.9968
		Time(s)	5.47	4.09	4.96	3.88
	40/ 16.09	PSNR(dB)	25.01	18.88	24.32	24.58
		SSIM	0.7186	0.6438	0.8900	0.9761
		Time(s)	5.53	4.01	4.55	3.84

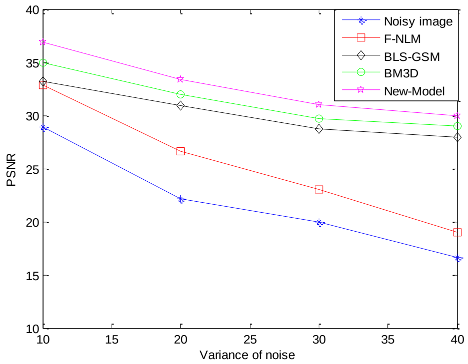

(a) Nxb

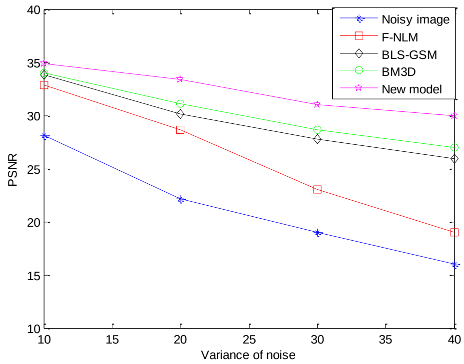

(b) Lib

Fig. 5. Simulated chart of PSNR of each model for noisy image（Nxb, Lib)

The peak signal-to-noise ratio de-noising simulation results of image Nxb and Lib, at different noise levels, is shown in fig 5. Above all experimental images and the data in Table 1 show that the F-NLM algorithm is faster, but sacrifices the denoising performance, which is inferior to other algorithms. It can be seen that among the three algorithms, the new model proposed in this paper has high peak signal-to-noise ratio and good structural similarity value, and the visibility is also the best. It not only effectively removes the noise interference, but also has certain information on the image edge structure information. Enhancement, controlling image information from local stability,

DOI: https://doi.org/10.34010/injiiscom.v7i1.15615
p-ISSN 2810-0670 e-ISSN 2775-5584

further confirms that the new model has ideal denoising performance.

3. CONCLUSION

In general, image restoration and the developments in this area are very crucial in the domain of image processing. The quality of the restored images will greatly affect their applications and uses in the community. Some of the possible sources of image degradation and restoration have been presented. However, many new strategies are still in their initial stages and hence more efforts will be made in order to move forward the developments.

In this piece of work, to balance the computing speed, denoising performance and to keep the complete the structural information of the image, the transform domain harmonic image filtering is used. To preprocess the noise added Image the three-dimensional block matching combined filtering is applied in addition to that, the high-frequency component of the pre-processed image i00s extracted for new model diffusion filtering. Finally, the frequency-domain component is reconstructed to obtain the final denoising effect. In order to avoid distortion when component reconstruction, Laplace Gauss algorithm is used to protect the edge-point spikes. There are numerous other algorithms for the Image Compression process, just like the one I have designed. So, what makes my project stand out?

Through the simulation experiments, we can see from the objective evaluation criteria and subjective visual effects that the internal information structure protection is more complete and the denoising performance is more idealized, which verifies the feasibility and superiority of the proposed algorithm and presents more information protection, and reasonable operation speed, which is beneficial to practical application. However, there’s always a room for improvement to attain way better results.

REFERENCES

Buades, A., Coll, B., & Morel, J. M. (2005, June). A non-local algorithm for image denoising. In *2005 IEEE computer society conference on computer vision and pattern recognition (CVPR'05)* (Vol. 2, pp. 60-65). Ieee.

Cornelis, B., Moonen, M., & Wouters, J. (2014). Reduced-bandwidth multi-channel Wiener filter based binaural noise reduction and localization cue preservation in binaural hearing aids. *Signal processing*, *99*, 1-16.

Dabov, K., Foi, A., Katkovnik, V., & Egiazarian, K. (2007). Image denoising by sparse 3-D transform-domain collaborative filtering. *IEEE Transactions on image processing*, *16*(8), 2080-2095.

Elad, M., Kawar, B., & Vaksman, G. (2023). Image denoising: The deep learning revolution and beyond—a survey paper. *SIAM Journal on Imaging Sciences*, *16*(3), 1594-1654.

Elmoataz, A., Desquesnes, X., & Lézoray, O. (2012). Non-local morphological PDEs and $ p $-Laplacian equation on graphs with applications in image processing

DOI: https://doi.org/10.34010/injiiscom.v7i1.15615
p-ISSN 2810-0670 e-ISSN 2775-5584

and machine learning. *IEEE Journal of Selected Topics in Signal Processing*, *6*(7), 764-779.

Fan, L., Zhang, F., Fan, H., & Zhang, C. (2019). Brief review of image denoising techniques. *Visual computing for industry, biomedicine, and art*, *2*(1), 7.

Foi, A., Katkovnik, V., & Egiazarian, K. (2007). Pointwise shape-adaptive DCT for high-quality denoising and deblocking of grayscale and color images. *IEEE transactions on image processing*, *16*(5), 1395-1411.

Hinton, G. E., & Salakhutdinov, R. R. (2006). Reducing the dimensionality of data with neural networks. *science*, *313*(5786), 504-507.

Hwang, H., & Haddad, R. A. (1995). Adaptive median filters: new algorithms and results. *IEEE Transactions on image processing*, *4*(4), 499-502.

Krizhevsky, A., Sutskever, I., & Hinton, G. E. (2012). Imagenet classification with deep convolutional neural networks. *Advances in neural information processing systems*, *25*.

LeCun, Y. (1989). Generalization and network design strategies. *Connectionism in perspective*, *19*(143-155), 18.

LI, W. G., & ZHAO, X. M. (2013). Multi-wavelet image denoising based on artifical bee colony algorithm. *Journal of Chongqing University of Posts and Telecommunication (Natural Science Edition)*, *25*(4), 532-537.

Mallat, S. G. (1989). A theory for multiresolution signal decomposition: the wavelet representation. IEEE transactions on pattern analysis and machine intelligence, 11(7), 674-693.

Perona, P., & Malik, J. (1990). Scale-space and edge detection using anisotropic diffusion. *IEEE Transactions on pattern analysis and machine intelligence*, *12*(7), 629-639.

Toprak, A., & Güler, İ. (2006). Suppression of impulse noise in medical images with the use of fuzzy adaptive median filter. *Journal of Medical systems*, *30*, 465-471.

Xian-Chun, Z., Mei-Ling, W., Lan-Fang, S., & Lin-Feng, Z. (2015). Diffusion denoising model based on the wavelet and biharmonic equation. *Acta Physica Sinica*, *64*(6).

Xie, J., Xu, L., & Chen, E. (2012). Image denoising and inpainting with deep neural networks. *Advances in neural information processing systems*, *25*.

Yuan, L., & Xu, X. (2015, August). Adaptive image edge detection algorithm based on canny operator. In *2015 4th International Conference on Advanced Information Technology and Sensor Application (AITS)* (pp. 28-31). IEEE.

DOI: https://doi.org/10.34010/injiiscom.v7i1.15615
p-ISSN 2810-0670 e-ISSN 2775-5584